Hopf Bifurcation in a Discontinuous Capacitor Voltage Mode Ćuk Dc-dc Converter

CORINA MIRELA IVAN*, DAN LASCU** and VIOREL POPESCU***
*Department of Applied Electronics
„Politehnica" University of Timisoara, Faculty of Electronics and Telecommunications
Bd. V. Parvan nr. 2 Timisoara
ROMANIA

**Department of Applied Electronics
„Politehnica" University of Timisoara, Faculty of Electronics and Telecommunications
Bd. V. Parvan nr. 2 Timisoara
ROMANIA

***Department of Applied Electronics
„Politehnica" University of Timisoara, Faculty of Electronics and Telecommunications
Bd. V. Parvan nr. 2 Timisoara
ROMANIA

Abstract – In this paper a simple closed-loop dc-dc Ćuk converter operating in Discontinuous Capacitor Voltage Mode (DCVM) is studied. Analysis of the state equations shows that the system loses stability via Hopf bifurcation. The results are verified through CASPOC simulation.

Keywords: Hopf bifurcation, chaos, Ćuk converter, dc-dc converters, averaged models, Discontinuous Capacitor Voltage Mode, power electronics.

1 Introduction

Occurrence of discontinuous modes in PWM dc-dc converters can be easily explained taking into account some topological aspects. In [1] it is shown that in every PWM converter the transistor and the diode form:

- a loop $\mathcal{L}$, with possibly the supply voltage, V_g, and a (possibly empty) set of capacitors;
- a cut-set $\mathcal{C}$, with a non-empty set of inductors.

In Discontinuous Capacitor Voltage Mode (DCVM) the small ripple assumption is invalid for at least one capacitor in the loop $\mathcal{L}$. A necessary and sufficient condition for the occurrence of DCVM is the existence of at least one capacitor in the loop $\mathcal{L}$, obviously different from the output filter capacitor. Therefore it is clear that DCVM cannot be related to Buck, Boost or Buck-boost converters, as these converters contain only a single capacitor for filtering the output voltage. On the other side, Ćuk, SEPIC and ZETA converters can enter DCVM mode when the small ripple assumption is removed from the energy storage capacitor contained in the loop $\mathcal{L}$.

Nonlinear phenomena in dc-dc converters have attracted considerable research attention in recent years [2], [3].

In [4] it is shown that the free-running current-controlled Ćuk converter, operating in continuous conduction mode (CCM), exhibits chaos via Hopf bifurcation.

In this paper the nonlinear behaviour of the dc-dc Ćuk converter operating in DCVM is studied. The averaged state equations are derived in Section 2. Based on the state equations, in Section 3 the stability of the system is analysed, revealing the supercritical Hopf bifurcation. The results are verified through CASPOC simulation. The simulation results are presented in Section 4.

2 Averaged State Equations

The system under study consists of a Ćuk converter, controlled by a simple proportional feedback scheme [6]. The duty cycle is given by:

$$d = D - \kappa(v_{C2} - V_{ref}) \quad (1)$$

where D is the steady-state duty cycle, κ is the feedback factor and V_{ref} is the voltage reference. A simplified schematic of the system is shown in Fig. 1.

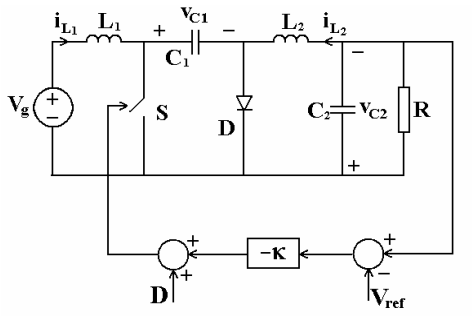

Fig. 1. The closed loop Ćuk converter.

2.1 Derivation of the state equations

The system can be described by the following state-space equations:

$$\begin{aligned}
\frac{dx}{dt} &= A_1 x + B_1 V_g, \qquad t_n \le t < t_n + d_1 T_s \\
\frac{dx}{dt} &= A_2 x + B_2 V_g, \quad t_n + d_1 T_s \le t < t_n + dT_s \quad (2) \\
\frac{dx}{dt} &= A_3 x + B_3 V_g, \quad t_n + dT_s \le t < t_n + T_s
\end{aligned}$$

where x is the state vector $[i_{L1}\ \ i_{L2}\ \ v_{C1}\ \ v_{C2}]^T$, $t_n = nT_s$, and T_s is the switching period. A and B for the three subintervals of a switching period are given by:

$$A_1 = \begin{bmatrix} 0 & 0 & 0 & 0 \\ 0 & 0 & \frac{1}{L_2} & -\frac{1}{L_2} \\ 0 & -\frac{1}{C_1} & 0 & 0 \\ 0 & \frac{1}{C_2} & 0 & -\frac{1}{RC_2} \end{bmatrix}; \quad B_1 = \begin{bmatrix} \frac{1}{L_1} \\ 0 \\ 0 \\ 0 \end{bmatrix} \quad (3)$$

$$A_2 = \begin{bmatrix} 0 & 0 & 0 & 0 \\ 0 & 0 & 0 & -\frac{1}{L_2} \\ 0 & 0 & 0 & 0 \\ 0 & \frac{1}{C_2} & 0 & -\frac{1}{RC_2} \end{bmatrix}; \quad B_2 = \begin{bmatrix} \frac{1}{L_1} \\ 0 \\ 0 \\ 0 \end{bmatrix} \quad (4)$$

$$A_3 = \begin{bmatrix} 0 & 0 & -\frac{1}{L_1} & 0 \\ 0 & 0 & 0 & -\frac{1}{L_2} \\ \frac{1}{C_1} & 0 & 0 & 0 \\ 0 & \frac{1}{C_2} & 0 & -\frac{1}{RC_2} \end{bmatrix}; \quad B_3 = \begin{bmatrix} \frac{1}{L_1} \\ 0 \\ 0 \\ 0 \end{bmatrix} \quad (5)$$

In order to derive the averaged state-space equations, the following assumptions are made: for the inductor currents, i_{L1} and i_{L2} the negligible ripple assumption is still valid, and therefore, they can be admitted equal to their averaged values and constant during one switching cycle; however, for the capacitor voltage, v_{C1} the small ripple assumption is not valid, while v_{C2} is assumed to be constant as in fact it is the output voltage. The capacitor voltage waveform v_{C1} is linear in the first and third subintervals because inductor currents are assumed to be constant during T_s, as mentioned above, and equal to zero in the second subinterval, as shown in Fig. 2, its expression in the first subinterval being given by:

$$v_{C1} = V_{pk}\left(1 - \frac{t}{d_1 T_s}\right) \quad (6)$$

and in the third subinterval:

$$v_{C1} = V_{pk}\frac{t - dT_s}{(1-d)T_s} \quad (7)$$

where the peak value of the capacitor voltage is equal to:

$$V_{pk} = \frac{\bar{i}_{L1}(1-d)T_s}{C_1} = \frac{\bar{i}_{L2} d_1 T_s}{C_1} \quad (8)$$

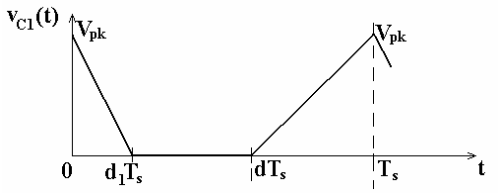

Fig. 2. The capacitor voltage v_{C1} waveform.

From Eqn.(8) the relative length of the first subinterval can be determined. Therefore:

$$d_1 = (1-d)\frac{\bar{i}_{L1}}{\bar{i}_{L2}} \quad (9)$$

By averaging the Eqn. (2) over T_s:

$$\frac{d\bar{x}}{dt} = \frac{1}{T_s}\int_0^{Ts} \frac{dx}{dt} dt \quad (10)$$

and using Eqns. (3)-(5), the Eqn. (10) becomes:

$$\begin{cases} \dfrac{d\bar{i}_{L1}}{dt} = \dfrac{1}{T_s}\left\{\int_0^{d_1 Ts}\dfrac{V_g}{L_1}dt + \int_{d_1 T}^{dTs}\dfrac{V_g}{L_1}dt - \int_{dT}^{Ts}\left(\dfrac{V_g}{L_1} - \dfrac{v_{C1}}{L_1}\right)dt\right\} \\ \dfrac{d\bar{i}_{L2}}{dt} = \dfrac{1}{T_s}\left\{\int_0^{d_1 Ts}\left(\dfrac{v_{C1}}{L_2} - \dfrac{v_{C2}}{L_2}\right)dt - \int_{d_1 T}^{Ts}\dfrac{v_{C2}}{L_2}dt\right\} \\ \dfrac{d\bar{v}_{C1}}{dt} = \dfrac{1}{T_s}\left\{-\int_0^{d_1 Ts}\dfrac{i_{L2}}{C_1}dt + \int_{dT}^{Ts}\dfrac{i_{L1}}{C_1}dt\right\} \\ \dfrac{d\bar{v}_{C2}}{dt} = \dfrac{1}{T_s}\left\{\int_0^{Ts}\left(\dfrac{i_{L2}}{C_2} - \dfrac{v_{C2}}{RC_2}\right)dt\right\} \end{cases} \tag{11}$$

By replacing Eqns. (6) and (7) into (11), the averaged state space model is found as:

$$\begin{cases} \dfrac{d\bar{i}_{L1}}{dt} = \dfrac{V_g}{L_1} - \dfrac{\bar{i}_{L1}(1-d)^2 T_s}{2L_1 C_1} \\ \dfrac{d\bar{i}_{L2}}{dt} = -\dfrac{\bar{v}_{C2}}{L_2} + \dfrac{\bar{i}_{L1} d_1 (1-d) T_s}{2L_2 C_1} \\ \dfrac{d\bar{v}_{C1}}{dt} = -d_1\dfrac{\bar{i}_{L2}}{C_1} + (1-d)\dfrac{\bar{i}_{L1}}{C_1} \\ \dfrac{d\bar{v}_{C2}}{dt} = \dfrac{\bar{i}_{L2}}{C_2} - \dfrac{\bar{v}_{C2}}{RC_2} \end{cases} \tag{12}$$

where by $\bar{x}$ is denoted the averaged (over a switching period) value of x.

For simplicity, let us consider that $L_1 = L_2 = L$.

As shown in [6], when converters are operating in discontinuous conduction mode the order of the system is reduced by one. Therefore, the Ćuk converter operating in DCVM is a third order system.

From Eqns. (1), (9), (12) the following state equations that describe the system dynamics result in:

$$\begin{cases} \dfrac{d\bar{i}_{L1}}{dt} = \dfrac{V_g}{L} - \dfrac{\bar{i}_{L1}\left(1 - D + \kappa(\bar{v}_{C2} - V_{ref})\right)^2 T_s}{2LC_1} \\ \dfrac{d\bar{i}_{L2}}{dt} = -\dfrac{\bar{v}_{C2}}{L} + \dfrac{\bar{i}_{L1}^2\left(1 - D + \kappa(\bar{v}_{C2} - V_{ref})\right)^2 T_s}{2LC_1\bar{i}_{L2}} \\ \dfrac{d\bar{v}_{C2}}{dt} = \dfrac{\bar{i}_{L2}}{C_2} - \dfrac{\bar{v}_{C2}}{RC_2} \end{cases} \tag{13}$$

These equations are valid only if $0 \le d \le 1$. To complete the model, the duty cycle saturation must be included:

$$\begin{cases} \dfrac{d\bar{i}_{L1}}{dt} = \dfrac{V_g}{L} - \dfrac{\bar{i}_{L1} T_s}{2L\ C_1} \\ \dfrac{d\bar{i}_{L2}}{dt} = -\dfrac{\bar{v}_{C2}}{L} + \dfrac{\bar{i}_{L1}^2 T_s}{2L\ C_1\bar{i}_{L2}}, \\ \dfrac{d\bar{v}_{C2}}{dt} = \dfrac{\bar{i}_{L2}}{C_2} - \dfrac{\bar{v}_{C2}}{RC_2} \end{cases} \quad \text{for } d<0 \tag{14}$$

$$\begin{cases} \dfrac{d\bar{i}_{L1}}{dt} = \dfrac{V_g}{L} \\ \dfrac{d\bar{i}_{L2}}{dt} = -\dfrac{\bar{v}_{C2}}{L} \\ \dfrac{d\bar{v}_{C2}}{dt} = \dfrac{\bar{i}_{L2}}{C_2} - \dfrac{\bar{v}_{C2}}{RC_2} \end{cases}, \quad \text{for } d>1 \tag{15}$$

The equilibrium point can be found by setting all the time derivatives to zero, resulting:

$$\begin{cases} I_{L1} = \dfrac{2C_1 V_g}{(1-D)^2 T_s} = \dfrac{V_g}{R_e} \\ I_{L2} = \dfrac{V_g}{R(1-D)}\sqrt{\dfrac{2C_1 R}{T_s}} = \dfrac{V_g}{\sqrt{RR_e}} \\ V_{C2} = \dfrac{V_g}{(1-D)}\sqrt{\dfrac{2C_1 R}{T_s}} = V_g\sqrt{\dfrac{R}{R_e}} = I_{L2}R \end{cases} \tag{16}$$

where X denotes the steady-state value of the state variable x, and:

$$R_e = \frac{(1-D)^2 T_s}{2C_1} \tag{17}$$

3 The Stability Of The System

The Jacobian matrix, *J(X)*, of the system, evaluated at the equilibrium point is given by:

$$J(X) = \begin{bmatrix} -\dfrac{R_e}{L} & 0 & -\dfrac{2V_g\kappa}{L(1-D)} \\ \dfrac{2\sqrt{RR_e}}{L} & -\dfrac{R}{L} & -\dfrac{1}{L} + \dfrac{2V_g\kappa}{L(1-D)}\sqrt{\dfrac{R}{R_e}} \\ 0 & \dfrac{1}{C_2} & -\dfrac{1}{RC_2} \end{bmatrix} \tag{18}$$

The eigenvalues (characteristic multipliers) of the Jacobian, *J(X)* can be found using the well known equation:

$$\det[\lambda I - J(X)] = 0 \tag{19}$$

Using Eqns. (16)-(18), Eqn (19) becomes:

$$\lambda^3+\left(\frac{1}{C_2R}+\frac{R+R_e}{L}\right)\lambda^2+$$
$$+\left[\frac{2}{C_2L}+\frac{R_e}{C_2LR}+\frac{RR_e}{L^2}-\frac{2\kappa V_g}{C_2L(1-D)}\sqrt{\frac{R}{R_e}}\right]\lambda+ \quad (20)$$
$$+2\left[\frac{R_e}{C_2L^2}+\frac{\kappa V_g\sqrt{RR_e}}{C_2L^2(1-D)}\right]=0$$

It is known that in order to exhibit Hopf bifurcation, the following conditions must be satisfied:

$$\mathrm{Re}(\lambda)\big|_{\kappa=\kappa_c}=0 \quad (21)$$

$$\mathrm{Im}(\lambda)\big|_{\kappa=\kappa_c}\neq 0 \quad (22)$$

$$\frac{d}{d\kappa}\mathrm{Re}(\lambda)\Big|_{\kappa=\kappa_c}\neq 0 \quad (23)$$

where κ_c is the critical value of κ at which a Hopf bifurcation occur.

4 Simulation Results

The investigated converter has the following circuit parameters: V_g = 10V, L = 10mH, R = 40Ω, C_1=56.8nF, C_2=11μF, f_s=20kHz, D=0.6.

The eigenvalues of the system, numerically calculated from Eqn. (20) for several values of the feedback factor (considered as bifurcation parameter) are shown in Table 1.

Form Table 1 it can be observed that, at κ=0.09449 the real part of the complex eigenvalues changes from negative to positive, while the imaginary part is not equal to zero, indicating a Hopf bifurcation.

Table 1. The characteristic multipliers

κ	The characteristic multipliers	Observations
0.07	-2540.7; -101.04±1041.7i	stable orbit
0.08	-2627.4; -57.7±1068.6i	stable orbit
0.09	-2708.2; -17.3±1092.8i	stable orbit
0.094	-2739.1; -1.8±1101.8i	stable orbit
0.09449	-2742.8; 0±1102.96i	Hopf bifurcation
0.095	-2746.7; 1.9±1104.1i	unstable orbit
0.1	-2784.1; 20.6±1114.8i	unstable orbit

The converter with the above mentioned circuit parameters was simulated in CASPOC. The scheme used for simulation is given in Fig. 3.

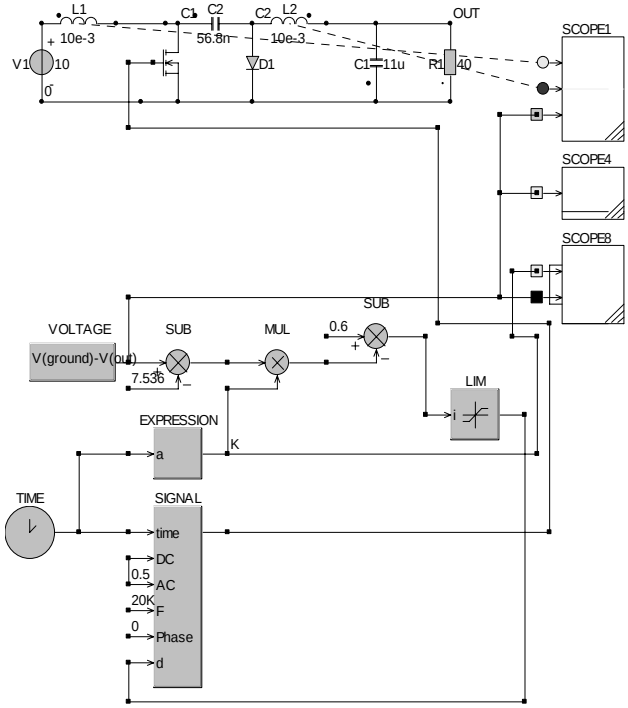

Fig. 3. The Ćuk converter scheme used in CASPOC simulation.

The bifurcation diagram, generated by CASPOC simulation is shown in Fig. 4.

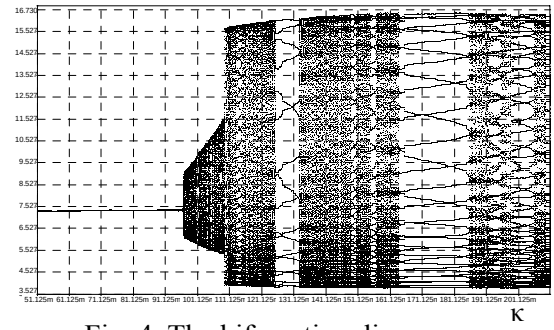

Fig. 4. The bifurcation diagram.

By simulating the closed-loop system, using CASPOC, it can be observed that:

- For small values of κ the trajectory is spiralling toward a fixed period-1 orbit. In Fig. 5 the trajectory, the stable period-1 orbit and the output voltage waveform are shown.
- The critical value κ_c, at which a Hopf bifurcation occurs, is found as 0.0945, which confirms the theoretical result.
- As κ increases, the orbit becomes unstable, settling into a limit cycle. The trajectory

spiralling away and the limit cycle are shown in Fig. 6.

- For even larger κ, the chaos occurs. The chaotic orbit is shown in Fig. 7.

The theoretical results obtained using the averaged space-state model are confirmed by the simulation.

The 3-D figures were obtained in MATLAB, by plotting the data exported from CASPOC simulation.

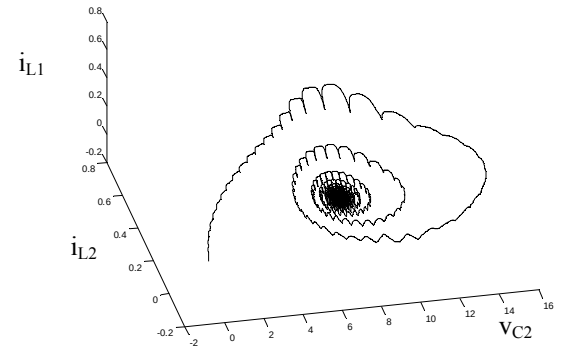

(a)

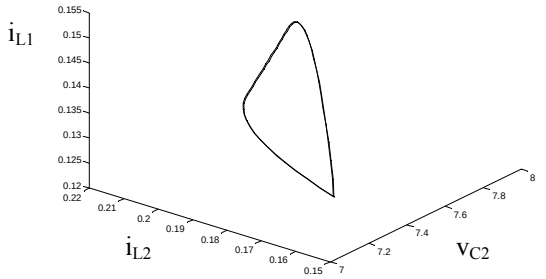

(b)

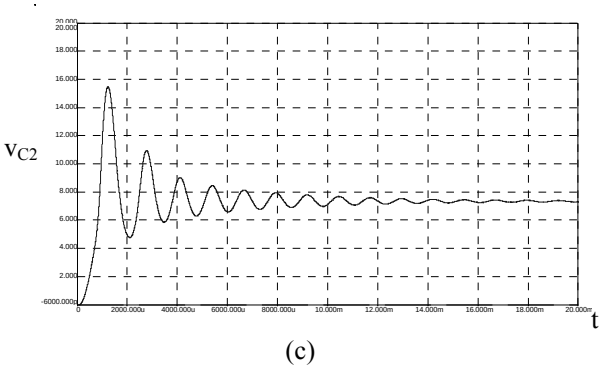

(c)

Fig. 5. Period-1 orbit: (a) the trajectory; (b) the stable period-1 orbit (κ=0.08); (c) the output voltage waveform.

The simulated trajectories presented in Fig. 5-7 show a Hopf bifurcation: the stable period-1 orbit becomes unstable and settles into a limit cycle, and finally becomes chaotic as the bifurcation parameter (the feedback factor) is increased.

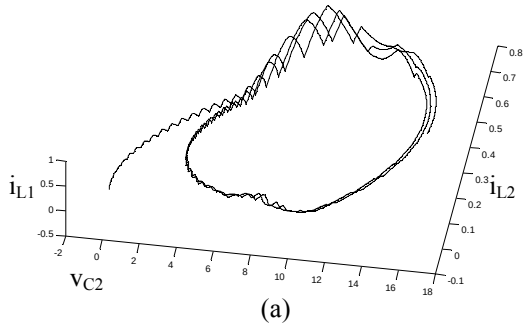

(a)

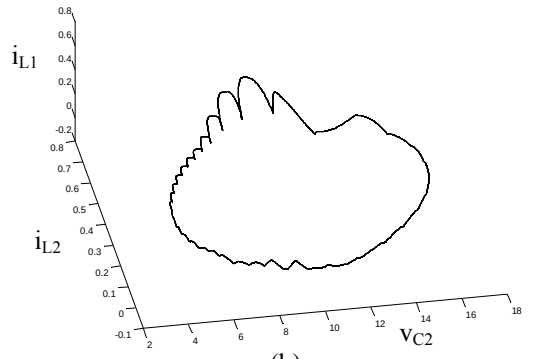

(b)

Fig. 6. Unstable period-1 orbit: (a) trajectory spiralling away; (b) limit cycle (κ=0.11).

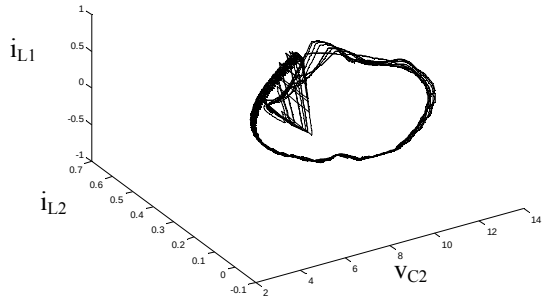

Fig. 7. Chaotic orbit (κ=0.3).

5 Conclusions

The power electronics circuits, due to their nonlinearity, exhibit a variety of complex behaviour.

In this paper the nonlinear behaviour of a simple feedback Ćuk dc-dc converter operating in discontinuous capacitor voltage mode (DCVM) was investigated. Using the averaged modelling, the stability of the system is studied. Based on the value of the characteristic multipliers of the system, it is shown that the Hopf bifurcation occurs at certain well estimated values of the feedback factor. The results are verified through CASPOC simulations. The bifurcation from a stable equilibrium orbit through limit cycles to chaos has been observed.

References

[1] D. Maksimović and S. Ćuk, A unified analysis of PWM converters in discontinuous modes, *IEEE Trans. Power Electron.,* Vol. 6, July 1991, pp. 476-490.

[2] J. H. B. Deane and D. C. Hamill, Instability, subharmonics, and chaos in power electronics circuits, *IEEE Transactions on Power Electronics*, Vol. 5, July 1990, pp. 260–268.

[3] S. Banerjee and G. C. Verghese, eds., *Nonlinear Phenomena in Power Electronics: Attractors, Bifurcation, Chaos, and Nonlinear Control*. IEEE Press, 2001.

[4] C. K. Tse, Y. M. Lai, and H. H. C. Iu, Hopf bifurcation and chaos in a free-running autonomous Ćuk converter, *IEEE Transactions on Circuits and Systems, Part I*, Vol. 47, April 2000, pp. 448–457.

[5] C. K. Tse, Flip bifurcation and chaos in three-state boost switching regulators, *IEEE Transactions on Circuits and Systems Part I,* Vol. 41, no. 1, 1994, pp. 16–23.

[6] C. K. Tse, *Complex Behaviour of Switching Power Converters*, CRC Press LLC, 2004.

[7] C. K. Tse, Chaos from a buck regulator operating in discontinuous conduction mode, *International Journal of Circuit Theory and Applications,* Vol. 22, 1994, pp. 263–278.

[8] P. T. Krein, J. Bentsman, R. M. Bass, and B. L. Lesieutre, On the use of averaging for the analysis of power electronic systems, *IEEE Transactions on Power Electronics*, Vol. 5, no. 2, Apr. 1990, pp. 192-192.

[9] D. C. Hamill, Power electronics: a field rich in nonlinear dynamics, *Proceedings of International Specialists' Workshop on Nonlinear Dynamics of Electronic Systems*, pp. 165–177, 1995.

[10] D. Lascu, P. van Duijsen, Discontinuous capacitor voltage mode dc-dc converters, *European Power Electronics Conference EPE-PEMC 2004, Riga, Letonia, 2004*.

[11] CASPOC - *Reference Manual*, Simulation Research, 1999.